

University of Massachusetts Dartmouth

Department of Physics

**Pion Photoproduction in the Energy Range between  
Threshold and the  $\Delta$ -Resonance Region**

A Thesis in

Physics

by

Kenneth A. Magno Jr.

Copyright 2008 by Kenneth A. Magno Jr.

Submitted in Partial Fulfillment of the

Requirements for the Degree of

Master of Science

January 2008

I grant the University of Massachusetts Dartmouth the non-exclusive right to use the work for the purpose of making single copies of the work available to the public on a not-for-profit basis if the University's circulating copy is lost or destroyed.

---

Kenneth A. Magno Jr.

Date \_\_\_\_\_

We approve the thesis of Kenneth A. Magno Jr.

Date of signature

---

Grant V. O’Rielly  
Assistant Professor, University of Massachusetts Dartmouth  
Thesis Advisor

---

William J. Briscoe  
Professor, The George Washington University  
Thesis Committee

---

Marguerite L. Zarrillo  
Professor, University of Massachusetts Dartmouth  
Thesis Committee & Chairperson, Department of Physics

---

Jianyi Wang  
Graduate Program Director, Department of Physics

---

Robert Peck  
Dean, College of Engineering

---

Richard J. Panofsky  
Associate Vice Chancellor for Academic Affairs and Graduate Studies

# ABSTRACT

## Pion Photoproduction in the Energy Range between Threshold and the $\Delta$ -Resonance Region

by Kenneth A. Magno Jr.

Studies of pion production reactions provide a way to test models of the nucleus based on quantum chromodynamics, QCD. These tests are possible since the creation of a pion from a nucleon requires an explicit rearrangement of the quarks. Due to the nature of the interactions, the photoproduction interaction is the least complex to model since there is no need to include Coulomb forces between the incident particles. At energies near threshold these results can be used to test Chiral Perturbation Theory. The experimental data is generally interpreted through partial wave analysis of the cross sections and angular distributions. Partial wave analysis is a technique by which information about the scattering amplitudes of the interaction can be determined. This research focuses on the  $\gamma + p \rightarrow n + \pi^+$  reaction. This reaction limits the need to model complex nucleon interactions in the nucleus. In the near-threshold range of 150 MeV to 175 MeV this reaction has not been extensively studied and the existing data sets contains very few points in this range. From the existing data set, partial wave analysis fits have been made with a number of different solutions. Due to sparse data in these low energy regions the existing solutions disagree. The purpose of the research described in this work is to utilize the MAID and SAID solutions to determine detector placement for a new experiment to be undertaken at MAX-lab in Lund, Sweden. The intention is to identify the best angles to place detectors in order to obtain data which will distinguish between the current PWA solutions in the energy range of 150 MeV to 180 MeV.

“Would you tell me, please, which way I ought to go from here?”

“That depends a good deal on where you want to get to,” said the Cat.

“I don’t much care where . . .” said Alice.

“Then it doesn’t matter which way you go,” said the Cat.

“ . . . long as I get somewhere,” Alice added as an explanation.

“Oh, you’re sure to do that,” said the Cat, “if you only walk long enough.”

Adventures of Alice in Wonderland. C.S. Lewis

## Acknowledgements

This work would not have been possible without the guidance and support of Dr. Grant V. O’Rielly, under whom I completed this thesis. I would also like to extend thanks to Dr’s. William J. Briscoe and Marguerite L. Zarrillo for their participation on my thesis committee. I would like to acknowledge the staff and faculty of the Physics Department at the University of Massachusetts Dartmouth for their contributions to my studies. In closing, I would like to thank my friends and family for their constant encouragement and support during my work on this thesis.

# Contents

## Chapter

<b>1</b>	Introduction	1
1.1	Synopsis . . . . .	1
1.2	History of the Pion . . . . .	3
1.3	Pion and the Quark Model . . . . .	5
1.4	Pion Production and Quantum Chromodynamics . . . . .	7
<b>2</b>	Pion Photoproduction	8
2.1	Advantages of Photoproduction Measurements . . . . .	8
2.2	Complications of Photoproduction Measurements . . . . .	9
2.3	Pion Photoproduction Reactions . . . . .	11
<b>3</b>	Pion Photoproduction Experiments	14
3.1	Generating Pions via Photoproduction . . . . .	14
3.2	Detecting Pions . . . . .	17
3.3	Previous Experiments . . . . .	19
<b>4</b>	Pion Photoproduction Theory	20
4.1	Chiral Perturbation Theory . . . . .	20
4.2	Partial Wave Analysis . . . . .	22
<b>5</b>	This Research	25

5.1 Experiment Overview . . . . . 25

5.2 Research Overview . . . . . 26

5.3 PWA Results . . . . . 30

    5.3.1 155 MeV . . . . . 30

    5.3.2 160 MeV . . . . . 31

    5.3.3 165 MeV . . . . . 32

    5.3.4 170 MeV . . . . . 32

    5.3.5 175 MeV . . . . . 33

    5.3.6 180 MeV . . . . . 35

5.4 Detector Placement . . . . . 35

    5.4.1 45 degrees . . . . . 36

    5.4.2 75 degrees . . . . . 36

    5.4.3 105 degrees . . . . . 37

    5.4.4 120 degrees . . . . . 37

5.5 Conclusions . . . . . 39

**Appendix**

**A** PWA Solutions at Incremental Energies . . . . . 41

**References** . . . . . 45

# Chapter 1

## Introduction

### 1.1 Synopsis

The pion is now understood to carry the strong nuclear force within the atomic nucleus, through the exchange of virtual pions between the nucleons in the nucleus. Since the pion can be described as a quark-antiquark pair, studies of pion production reactions provide a way to test models of the nucleus based on quantum chromodynamics, QCD [1]. These tests are possible since the creation of a pion from a nucleon requires an explicit rearrangement of the quarks. The pion can be observed when it is created in a number of different ways; nucleon-nucleon, electron-nucleon, and photon-nucleon interactions. These interactions can be modeled to gain a better understanding of not just the pion but the nucleus as well. Due to the nature of the interactions, the photoproduction interaction is the least complex to model since there is no need to include Coulomb forces between the incident particles. Experimental results from such measurements can be used to test the predictions from QCD models against measurements. At energies near threshold these results can be used to test Chiral Perturbation Theory [1]. The experimental data is generally interpreted through partial wave analysis of the cross sections and angular distributions. Partial wave analysis is a technique by which information about the scattering amplitudes of the interaction can be determined. This allows for the interaction to be exam-

ined in terms of the angular momentum and is generally restricted to s-wave ( $\ell = 0$ ) and p-waves ( $\ell = 1$ ) [2], particularly at low energies since their contributions will be dominant.

For pion photoproduction the threshold energy is approximately 150 MeV, and the photon can interact with either the proton or neutron. Consequently, there are four channels by which pion photoproduction can occur; neutral pion productions  $\gamma + p \rightarrow \pi^0 + p$  or  $\gamma + n \rightarrow \pi^0 + n$ , and charged pion production  $\gamma + n \rightarrow \pi^- + p$  or  $\gamma + p \rightarrow \pi^+ + n$ . For the neutral channels, the  $\gamma + p \rightarrow p + \pi^0$  reaction has been extensively investigated [3] while the other reaction  $\gamma + n \rightarrow n + \pi^0$  is experimentally difficult to perform. For the charged channels, the  $\gamma + n \rightarrow \pi^- + p$  is difficult to perform since there is no neutron target available, deuteron targets have been substituted in experiments for the reaction  $\gamma + d \rightarrow \pi^- + p + p$ , however the inverse reaction,  $\pi^- + p \rightarrow \gamma + n$  has been studied. The focus of this research, the  $\gamma + p \rightarrow n + \pi^+$  reaction, is relatively straightforward to study since hydrogen can be used as a proton target. This limits the need to model complex nucleon interactions in the nucleus. Additionally, in the near-threshold range of 150 MeV to 175 MeV this reaction has not been extensively studied and the existing data sets contains very few points in this range. Between 154 MeV and 180 MeV there is no modern data for this process. From the existing data set, partial wave analysis fits have been made with a number of different solutions. The two major analysis are MAID [4], from the Mainz University in Germany, and SAID [5], from George Washington University in Virginia. However, due to sparse data in these low energy regions the existing solutions disagree.

The purpose of the research described in this work is to utilize the MAID and SAID solutions to determine detector placement for a new experiment to be undertaken at MAX-lab in Lund, Sweden. The recently upgraded tagged photon facility can now provide photon energies up to 200 MeV permitting the study of pion photoproduction reactions. The intention is to identify the best angles to place detectors in order to

obtain data which will distinguish between the current PWA solutions in the energy range of 150 MeV to 180 MeV. The planned precision of the measurements will produce data at specific angles to assist in determining which of these various solutions best describes the  $\gamma, \pi^+$  data. This data will also improve the partial wave solutions from SAID and MAID in the energy range between threshold and the first resonance region.

## 1.2 History of the Pion

Hideki Yukawa was the first to propose the existence of a meson as the exchange particle for the strong nuclear force in 1935 [6]. Originally called a mesotron, from “meso” meaning middle, since their mass was believed to lie between that of the known light particle such as electrons and the heavy nucleons. Yukawa was attempting to explain why the strong nuclear force has a limited range of about 1 fm, whereas the electromagnetic and gravitational forces have an infinite range. Using this known 1 fm range, and the fact that the particle could only exist if it did not violate conservation of energy it can be determined from the Heisenberg uncertainty principle that  $x = ct = \hbar c / mc^2$ . Assuming that the range of the nuclear force would be  $k^{-1} = \hbar / mc$ , Yukawa determined that the particle would have a mass of about 100 MeV/c<sup>2</sup>.

Particle accelerators of the mid 1930’s and early 1940’s were not of sufficiently high energy to generate the predicted mesons for experiments. Most of the early searches for these mesons came from studying photographic emulsions at high altitudes. The photographic emulsions were lifted high in the atmosphere where it was believed that high energy cosmic rays entering the atmosphere could produce these mesons through collisions with nucleons. Between 1936 and 1937 the first tentative observation of a meson using these photographic emulsions was made by S. H. Neddermeyer and C. Anderson [7]. The particles they observed had a mass of just over 100 MeV/c<sup>2</sup>, and was believed to be close enough to the prediction by Yukawa to be the predicted

exchange meson. Additional studies determined that these particles had a range which was greater than would be expected for the predicted exchange particle: if it were the exchange particle for the nuclear force it should interact strongly with nuclei and should have a very short range in matter. What had been discovered was called the  $\mu$ -meson, and is now known as a muon. Later it was determined that the muon was not a meson but rather a lepton closely related to the electron. Bethe and Marshak studied this newly discovered particle and hypothesized that the muon could still be connected to the strong nuclear force, resulting from the decay of Yukawa's exchange meson [8].

Work continued in the search for Yukawa's meson, however it was not until 1947 that there were conclusive observations. In 1947, C.F. Powell and his collaborators discovered what they identified as two distinct particles in emulsion tracks on photographic plates [9]. One particle had a mass of about  $150 \text{ MeV}/c^2$  while the second particle had a mass of about  $100 \text{ MeV}/c^2$ . The lighter particle was the muon which had been discovered a decade earlier. The heavier particle was the exchange meson proposed by Yukawa. The particle was called a  $\pi$ -meson or pion. From studies of the photographic emulsions, it was determined that there were two different pions, a positively charged pion ( $\pi^+$ ) and a negatively charged pion ( $\pi^-$ ). Modern understanding of pion decay is that charged pions decay most commonly, more than 99% of decays, into muons. These reactions,  $\pi^+ \rightarrow \mu^+ + \nu_\mu$  and  $\pi^- \rightarrow \mu^- + \bar{\nu}_\mu$ , have a lifetime of approximately 26 ns. The hypothesis of Bethe and Marshak that the muon was in fact the decay product of the charged pion had been confirmed.

A year later, in 1948, the team of C.M.G. Lattes at the University of California in Berkeley were able to artificially produce pions using a cyclotron. By bombarding a carbon target with 380 MeV alpha particles which had been accelerated in the cyclotron they were able to artificially create and observe pions. The work at the University of California in Berkeley continued and in 1950 neutral pions,  $\pi^0$ , were

detected. Since the neutral pion leaves no tracks in a photographic emulsion, to be identified the  $\pi^0$  was identified by its double-photon decay,  $\pi^0 \rightarrow \gamma\gamma$ , from which the photons will produce tracks. As synchro-cyclotron facilities used to produce pions evolved, dedicated laboratories such as CERN near Geneva, Switzerland, LAMPF in Los Alamos, NM, and TRIUMF in Vancouver, British Columbia were built and became known as *meson factories*. These facilities use intense high energy proton beams to produce pions in such great quantities that beams of pions could be extracted and used to study the interactions of pions with various nuclear targets.

### 1.3 Pion and the Quark Model

The modern model describing the nucleus and nucleons is the quark model, based on QCD. In the quark model, nucleons are made up of three quarks, each of which carry fractional charge. The up quark,  $u$ , has a charge of  $+2/3$  and the down quark,  $d$ , has a charge of  $-1/3$ . In this model the proton, denoted  $uud$ , is made up of two up quarks with charge  $+2/3$  each and one down quark with charge  $-1/3$ , thus the net charge of the proton is  $+1$ . Neutrons,  $udd$ , have neutral charge from being made from two down quarks with charge  $-1/3$  each and one up quark with charge  $+2/3$ . In the quark model, pions can be described as a quark anti-quark pair,  $q\bar{q}$ .

Pion creation occurs through the collision of energetic particles, where the energy of the collision can create a quark anti-quark pair,  $q\bar{q}$ . From this quark anti-quark pair, along with the three quarks of the nucleon, a pion is formed. This pair including an anti-quark allows for the creation of the two quark pion as opposed to three quarks in a nucleon. The  $\pi^+$  is made up of an up quark of charge  $+2/3$  and an anti-down quark of charge  $+1/3$ , which is written as  $u\bar{d}$ . This gives the  $\pi^+$  the same charge as a proton. Formation of the  $\pi^-$  is from a down quark of charge  $-1/3$  and an anti-up quark of charge  $-2/3$ , which is written as  $\bar{u}d$ . Thus a  $\pi^-$  has the same charge as an electron. The neutral pion,  $\pi^0$ , is a more complex situation. A  $\pi^0$  can be formed from

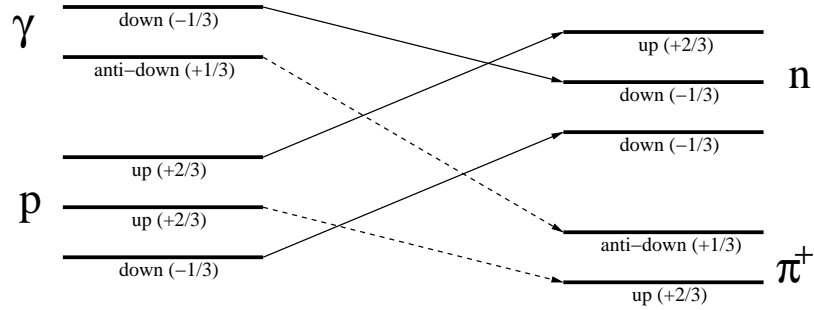


Figure 1.1: Quark rearrangement in  $\gamma + p \rightarrow \pi^+ + n$  interaction

an up quark and anti-up quark,  $u\bar{u}$ , or a down quark and anti-down quark,  $d\bar{d}$ . Since both arrangements contribute to the structure of the  $\pi^0$  it is commonly written as the superposition of both possibilities,  $u\bar{u} + d\bar{d}/\sqrt{2}$ .

Through the study of pion photoproduction it is possible to gain understanding of the quark model. This is due to the fact that in pion production there is a rearrangement of the quarks which occurs since nucleons are made from three quarks,  $qqq$ , and the pion is made up of a quark anti quark pair,  $q\bar{q}$ . For the case of  $\gamma + p \rightarrow \pi^+ + n$ , shown in Fig. 1.1, the photon can be viewed as a  $d\bar{d}$  pair and the proton as being  $uud$ . The resulting neutron is an  $udd$  and the  $\pi^+$  is a  $u\bar{d}$  where the photon pair has been split between the two products and one of the quarks from the proton has become part of the  $\pi^+$ .

The  $\pi^+$  and  $\pi^-$  both have a mass of  $139.6 \text{ MeV}/c^2$  and the  $\pi^+$  and  $\pi^-$  are considered to be a particle anti-particle pair. The  $\pi^0$  has a slightly lower mass of  $135.0 \text{ MeV}/c^2$ , which is attributed to the  $\pi^0$  having no charge. The  $\pi^0$  is considered to be its own anti-particle. The lifetimes of the free  $\pi^+$  and  $\pi^-$  are both  $2.6 \times 10^{-8} \text{ s}$ . A  $\pi^0$  has a significantly shorter lifetime, or half-life, of  $8.4 \times 10^{-17} \text{ s}$ . Using these lifetimes and assuming that pions move at a maximum possible speed of the speed of light,  $3 \times 10^8 \text{ m/s}$ , the maximum range before decay can be calculated and explain why direct detection of  $\pi^0$  is nearly impossible. For the  $\pi^+$  and  $\pi^-$  the distance traveled would be 7.8 m before half of the pions decay. On the other hand, the  $\pi^0$  would travel

about 25 nm before half of the pions decay. In the distance it would take created  $\pi^\circ$  to travel to a detector, the total number of  $\pi^\circ$  incident to the detector would almost be non-existent. With such a short range before decay, the  $\pi^\circ$  is detected by its decay products instead of directly.

## 1.4 Pion Production and Quantum Chromodynamics

As noted earlier, in the quark model, pion creation involved the rearrangement of quarks. One of the most important connections which needs to be made by modern science is between nucleons and the theoretical framework provided by QCD [10]. One of QCD focuses is describing the interaction between quarks and gluons to form hadrons. Quarks however seem to exist only as combinations of three quarks in baryons, or as quark and anti-quark pairs in mesons [10]. The pion is considered to be one of the simplest quark systems available to study, which makes pion photoproduction a very desirable process to further the understanding of QCD and quark models. It is believed that to meet this goal of modern science, and to better understand the strong nuclear force, it is necessary to study pion photoproduction as well as other elementary particle reactions [1]. Pion photoproduction involved the explicit rearrangement of quarks in the nucleon. The study of this reaction will directly address this needed connection.

## Chapter 2

### Pion Photoproduction

#### 2.1 Advantages of Photoproduction Measurements

Since the laboratory production of pions began in the late 1940's and early 1950's there have been two fundamental mechanisms through which to investigate the pion; nucleon-nucleon collisions and photon-nucleon collisions, also known as photoproduction. Though electron-nucleon collisions, electroproduction, can also produce pions interacting with the nucleon. This process can be reduced to a photoproduction with a virtual photon. Photoproduction has several advantages: first, the photon-nucleon collision involves only one nucleon as opposed to the nucleon-nucleon collision which involves two nucleons. This means the photon-nucleon collision is a first order process with the cross section being related to  $g^2$ , where  $g$  is the meson-nucleon coupling constant [11]. The nucleon-nucleon collision is a third order process, which complicates the process of pion creation. Thus, the uncertainty for the photon-nucleon collision predictions is less since it is a first order process. Second, with nucleon-nucleon collisions, some assumptions must be made for perturbation calculations of the pion with respect to the character of the virtual meson field where the collision occurs. Basically, it matters whether it is assumed that the pion alone is responsible for the strong nuclear force, or if it is assumed that other meson fields contribute along with the pion to the nuclear force. Photoproduction has a saving grace in the lowest order

of perturbation theory, only the pion field is considered to be involved. This allows the higher order corrections to be neglected. Another advantage of photoproduction over nucleon-nucleon collision comes about from the fact that the photon is absorbed in the process. Since the final state of photoproduction only consists of a nucleon and a meson, the system is a simple two-body problem. Nucleon-nucleon collisions become a three-body problem since the final state contains two nucleons and a meson. Furthermore, the nucleons can distort the high energy end of the pion spectrum due to strong interactions, with the outgoing pion distortion complicating comparison between the theory and experiment [11].

## 2.2 Complications of Photoproduction Measurements

Pion photoproduction compared with the closely related process electroproduction does have one disadvantage, which has to do with the production of the photons. This takes into account the strength of the strong interaction and introducing nuclear physics reaction regime energies of a few MeV. Pion production has a threshold energy of about 150 MeV. Producing photons of these energies is typically done using high energy electrons to produce bremsstrahlung photons. A detailed description of the bremsstrahlung process can be found in Chapter 3. Due to the nature of the bremsstrahlung process, the photons produced will have energies which range from zero up to a maximum energy equal to that of the incident electron energy. Since bremsstrahlung photons are not monoenergetic in experiments, which electrons can be, experimentally we deal with the uncertainty  $\frac{d\omega}{\omega}$  where  $\omega$  is the energy of the photon. This comes about due to the spectrum characteristics of bremsstrahlung radiation which is used to produce the photon beams. The experimental results can be expressed in terms of the photon energies which are unique when the energies and angles of the pion and the recoil nucleon are measured [11]. The measurement of the recoil neutron is however difficult since it relies on the neutron getting out of the tar-

get to be measured. This however cannot allow for the assumption of monoenergetic photons to be used when the individual photon energies are determined.

In the past, the endpoint subtraction method was used to determine the cross sections for bremsstrahlung experiments. This process was done using normalized plots of the number events per bremsstrahlung energy from two known electron beam energies,  $E_1$  and  $E_2$ . From these plots, only towards the higher energy bremsstrahlung end of the plots would the two plots differ. Considering the area under each plot to be the total cross section for that energy, by subtracting the two plots it would be possible to determine the energy differential cross section of the higher energy plot. Thus, the difference

$$\sigma_{\text{total}}(E_2) - \sigma_{\text{total}}(E_1) \simeq \frac{d\sigma}{dE}(E_2)$$

This process assumes that the flux at the two endpoint energies  $E_1$  and  $E_2$  is the same. The uncertainty in the flux determination for bremsstrahlung experiments is typically 10% – 20%. This is due to the fact that with any counting experiment the uncertainty in  $N$  is  $\sqrt{N}$ , and for differences  $\Delta(E_2 - E_1) = \sqrt{E_2 + E_1}$  with these energies. This disadvantage can be overcome in some specific situations due to the two-body characteristics of photoproduction. One additional complication of electroproduction over photoproduction is that the cross sections are smaller. Electroproduction cross sections are smaller by an of the fine structure constant,  $\alpha$ , in calculations.

## 2.3 Pion Photoproduction Reactions

For pion photoproduction there are four possible reactions which may occur. These reactions are:

$$\gamma + n \rightarrow \pi^0 + n$$

$$\gamma + n \rightarrow \pi^- + p$$

$$\gamma + p \rightarrow \pi^0 + p$$

$$\gamma + p \rightarrow \pi^+ + n$$

The first two reactions, which involves a photon interacting with a neutron, must be studied indirectly since there is no free neutron target. These  $\gamma + n$  interactions are typically studied by using the deuteron as the target nuclei [2] and accounting for nuclear effects of the target in the reaction through calculations. Another way to study the  $\gamma + n \rightarrow \pi^- + p$  reaction is through the inverse-capture reaction  $\pi^- + p \rightarrow \gamma + n$ . Both of the  $\gamma + p$  interactions can be studied directly since proton targets can easily be obtained using hydrogen. The cross sections of these interactions are simplest at energies near threshold. As higher energy photons are incident on the nucleons, the nucleons can transition into higher energy states. This produces nucleon resonance states which complicate the interpretation of the cross sections. Resonances occur when a nucleon gains enough energy to make a transition into an excited state,  $\gamma N \rightarrow N^*$ . The lowest energy resonance is known as the  $\Delta(1232)$  resonance; designated as the  $P_{33}$  nucleon state it has a spin parity  $J^\pi = \frac{3}{2}^+$ , an isospin  $T = \frac{3}{2}$ , and an  $\ell_\pi = 1$  which corresponds to a p-wave [12].

Pion photoproduction can be viewed as occurring through various unique interactions. These interactions are commonly represented by the use of Feynman diagrams, shown in Figure 2.1 below. Six different Feynman diagrams are shown which represent the  $\gamma + p \rightarrow \pi^+ + n$  interaction.

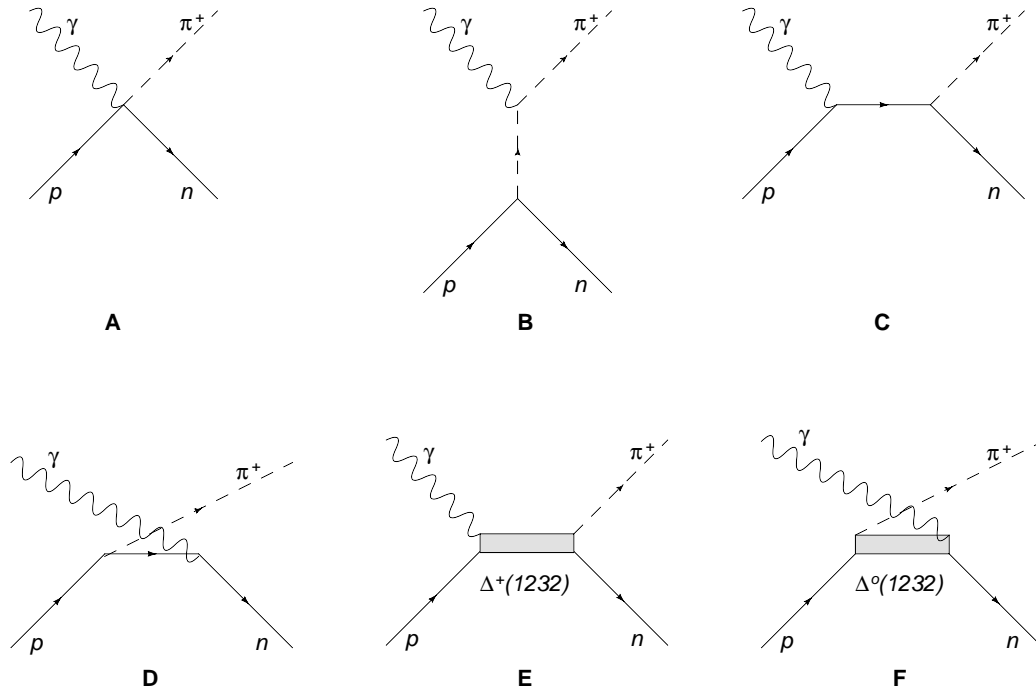


Figure 2.1: The Feynman diagrams of the  $p(\gamma, \pi^+)n$  reaction

In the diagrams of Figure 2.1 :

- A:** The photon couples directly to the proton and the  $\pi^+$  is produced at the same vertex. Diagram A is sometimes called the Seagull diagram or the Kroll-Rudermann term [12]. At and near threshold this interaction contributes solely to the s-wave photoproduction of the  $E_{0+}$  multipole which dominates the cross section for charged pion production.
- B:** A photon couples to the charge of a virtual  $\pi^+$  without direct contact with the proton. This interaction, designated as the t-channel, contributes to both the s-wave and p-wave photoproduction of all multipoles.
- C:** The s-channel is a photon coupling with a proton and generating a  $\pi^+$  at a second vertex. This also contributes to s-wave and p-wave photoproduction of the  $E_{0+}$  and  $M_{1-}$  multipoles.

- D:** A proton emits a  $\pi^+$  and the photon then couples with the neutron. This is known as the u-channel, which can generally be ignored. The u-channel contribution with respect to the s-channel of Diagram C is small since the reaction occurs via the photon interacting with the magnetic moment of the neutron [12].
- E:** A photon interacts with a proton causing the proton to make a transition into the  $\Delta^+(1232)$  resonance state. The excited state then decays into the  $\pi^+$  and a neutron. The contribute of this interaction, designated as the  $\Delta$  s-channel, is to the p-wave photoproduction of the  $M_{1+}$  and  $E_{1+}$  multipoles.
- F:** A proton decays to the  $\Delta^0(1232)$  resonance state and a  $\pi^+$ . Then a photon interacts with the neutron. Called the  $\Delta$  u-channel, it is similar to Diagram D and its contribution is considered to be small.

## Chapter 3

### Pion Photoproduction Experiments

#### 3.1 Generating Pions via Photoproduction

The most common process for performing photoproduction experiments has been through the use of bremsstrahlung beams. Bremsstrahlung, from the German for “braking radiation”, occurs when an incident charged particle, typically an electron, is deflected by another charged particle, commonly a nucleus. Due to the acceleration of the electron during its change in direction it emits electromagnetic radiation, the energy of which will depend on the energy of the incident electron and the angle at which it is deflected. With a sufficiently intense electron beam, a large number of photons can be created. In most photoproduction experiments the incident particle is an electron which has been accelerated in a linear accelerator, LINAC, to a known energy. Once the electron interacts with the radiator, the photons created will have a range of energies, thus the photon beam is not monochromatic. To ensure that the unconverted incident electrons do not interfere with the experiment, a magnetic field, known as a dump magnet, bends the incident electrons away from the target and into a well shielded beam dump. Finally, the photon beam passes through the collimator to define the beam size which will interact with the target of the experiment.

Bremsstrahlung photon experiments can have a myriad of problems. First off, the wide range of photon energies can result in incomplete kinematics for the exper-

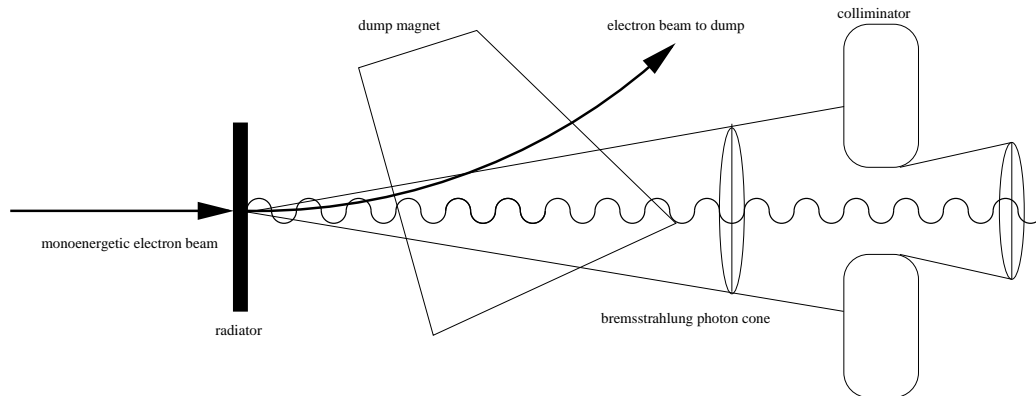


Figure 3.1: Bremsstrahlung Photon Generation

iment. The incident photon energy is not known for any single event, consequently a detected low energy particle may have been produced by a low-energy photon or a high-energy photon plus some final state interactions which degraded the reaction product into the detected low-energy particle [12]. There have been some attempts in the 1970's to extract the monoenergetic contribution of the photon flux through various techniques but, these calculations were susceptible to large systematic and statistical uncertainties. For bremsstrahlung experiments the total number of photons incident upon the target is not easily determined. Furthermore, there is no timing for the incident photon when using bremsstrahlung. These complications of standard bremsstrahlung have lead to the development in photon tagging.

Photon tagging begins with a standard bremsstrahlung beam being generated. However, the electrons are not all sent off to a beam dump after generating photons. The magnet is used to extract the post-bremsstrahlung electrons from those which did not interact with the radiator target. The magnet deflects the post-bremsstrahlung electrons towards a detector array located along the focal plane of the magnet. The detectors commonly are scintillation detectors as these can handle the high rates typically required for these experiments. The position of the scintillation counter and the magnetic field strength will determine the momentum of the post-bremsstrahlung electron [13]. Thus, the energy of the post-bremsstrahlung electron can be determine

from the momentum measurement. Consequently, through conservation of energy,  $E_\gamma = E_{e_{\text{incident}}} - E_{e_{\text{post-brem}}}$ , so the photon energy is known. Additionally, a time signal can be generated for the photon enabling coincidence experiments. The flux of photon passing through the production target is provided directly by counting the number of post-bremsstrahlung electrons, and the energy of the photon is known [13]. Any additional electrons which did not interact with the radiator material bend towards a beam dump due to their energy being greater than that of a post-bremsstrahlung electron. Since the post-bremsstrahlung electrons are counted the photon in the beam produced can be considered to have been counted at their single energy. For the bremsstrahlung process however, the beam passes through a collimator so this count is not the exact number of photons incident to the target.

There are many research facilities capable of performing tagged photon experiments. One facility which has performed tagged photon experiments is the Saskatchewan Accelerator Laboratory, SAL, now part of the Canadian Light Source. SAL was capable of obtaining energies photon up to 300 MeV. Another is the Mainz Microtron, MAMI, at the Johannes Gutenberg University of Mainz in Germany where of energies up to 1.5 GeV can be obtained. In the United States one facility of interest for tagged photon experiments is Thomas Jefferson National Accelerator Facility, known as Jefferson Lab or JLab, in Newport News, VA. Jefferson Lab is currently undergoing an upgrade to allow energies up to 12 GeV. The tagged photon facility related to this research is MAX-lab at Lund University in Sweden where the proposed measurements will take place. MAX-lab is capable of operating at energies up to 1.5 GeV and operates 14 beam lines and three storage rings, including 250 MeV tagged photon facility for nuclear physics research.

There are other methods for generating tagged photons such as Compton back scattering of laser light from a high-energy electron beam. The Grenoble Anneau Accélérateur Laser, GRAAL, at the European Synchrotron Radiation Facility in Greno-

ble, France has done work with Compton back scattering experiments. Other facilities capable to perform Compton back scattering experiments include Spring-8 in Japan and LEGS, the Laser Electron Gamma-ray Source, located at Brookhaven National Laboratory in Upton, NY.

### 3.2 Detecting Pions

Since pion photoproduction experiments began around 1950 there have been several techniques developed to detect pions and their products. The earliest is referred to as the  $\pi^+$ ,  $\mu^+$ ,  $e^+$  method. The pion and the muon are stopped in the target. Then the  $e^+$  which the muon decays into is detected. Since the muon has a lifetime of  $2.2 \mu s$ , the count is made after the beam pulse which helped to reduce background problems [13]. The Saclay-Louvain collaboration created this method which is only usable for detecting  $\pi^+$  up to 30 MeV above threshold on light nuclei. A second method which was introduced in 1957 by Hughes and March is known as the Activity Method. In this case, the radioactivity of the residual nucleus is detected. Most of the common reactions for this method used carbon, lithium, boron, oxygen, or nitrogen as the target nuclei. One of the more favorable reactions is  $^{12}\text{C}(\gamma, \pi^-)^{12}\text{N}$  since it only has one bound state. For  $\pi^+$  generation one possible reaction is multiple excited bound states is  $^{16}\text{O}(\gamma, \pi^+)^{16}\text{N}$ . Unfortunately, background problems as well as effects of the Coulomb barrier cause  $\pi^+$  to have low cross sections. Thus, the only two major experiments performed by the Activity Method both were for  $\pi^-$  near threshold [13].

The most beneficial method of pion detection has been pion spectrometers. The largest benefit of this method is that it allows for the measurement of differential cross sections, which provide more sensitive tests of theoretical predictions than is possible by total cross sections. Additionally, pion spectrometers allow for the variance of energy and momentum transfer separately. Due to this fact various components of the photoproduction process can be individually tested. As previously noted,

monochromatic photon sources do not occur since bremsstrahlung beams are used in photoproduction experiments. It is necessary to use bremsstrahlung photons in order to obtain sufficient count rates to perform an experiment. Thus instead of discrete lines, staggered yield curves are obtained, one for each excited state [13]. In most cases, resolution of states is limited by these curves to approximately 1 MeV, though up to 100 keV resolution is possible through analysis.

Another common observation method for pions involves the use of scintillator detectors. In scintillator detectors the energetic particle enters into a material, a scintillator, where the particle interacts causing the atoms of the material to be excited due to the energy deposited by the particle. The excited atoms then rapidly emit light and the material is said to fluoresce [12]. The emitted light interacts with a photosensitive material in a photomultiplier tube, turning the light signal into a group of electrons. The photomultiplier tube amplifies the electric pulse caused by the electrons by accelerating them and producing secondary electrons. From this electric pulse, information about the energy of the incident particle can be determined. The scintillator can be made of various materials such as inorganic crystals, organic liquids, organic solids, or plastics. Plastic scintillator material has the benefit of being easily cut and formed into desired shapes and sizes. Using plastic scintillators, detectors can be constructed which can aid in particle identification. This can be done by having the incident particle pass through a thin plastic scintillator detector, depositing a small amount of energy, then entering a second plastic scintillator detector large enough to stop the particle completely. From the amount of energy deposited in the thin detector and knowing the total energy deposited in both detectors the particles can be identified and its energy known.

### 3.3 Previous Experiments

Though pions have been artificially produced using cyclotrons since 1948, it was not until the early 1970's that low energy pion photoproduction experiments began to be performed. The first experiments were performed at the Saclay electron LINAC, by a collaboration from Louvian University, and at the Bates LINAC [14]. A major motivation at the time for studying low energy pion photoproduction was the recognition that it was a promising tool for studying specific details in nuclear structure. By 1977 enough new electron LINACs were in operation such that accurate experimental data was beginning to appear. The interest in pion photoproduction continued to grow after the first international conference on Photopion Nuclear Physics in 1978 [13]. Experimental data for pion photoproduction gained some of its greatest improvements around this time. Many of the new electron LINACs were high duty-cycle and high intensity, which made it possible for the first time to investigate in detail the transitions to individual levels. Facilities including Bates, Mainz, and Saskatchewan installed magnetic pion spectrometers, a high resolution spectroscopic tool. Pion spectrometers benefited from the improved statistics that the high beam currents that the new LINACs provided. A majority of the experiments carried out during the late 1970's and into the 1980's, however, still relied on bremsstrahlung beams of untagged photons to insure high statistics. The few tagged photon experiments which occurred during the 1980's and into the 1990's generally were measured in low-statistics experiments and thus had large energy and angular binning. A majority of the tagged data was of excitation cross sections with no extensive angular range [3].

## Chapter 4

# Pion Photoproduction Theory

### 4.1 Chiral Perturbation Theory

In the early 1970s pion photoproduction threshold amplitudes were predicted using a Low Energy Theorem (LET) which was derived by de Baenst, Vainshtein, and Zakharov [15]. This LET was based on fundamental principles including Lorentz and Gauge invariance, and chiral symmetry. The form of the LET power series includes the variable  $\mu = \frac{m_\pi}{m_N}$  where  $m_\pi$  and  $m_N$  are the mass of the pion and nucleon, respectively. The discrepancy between the experimental data and the LET predictions was based on the assumption that the amplitudes would be functions of  $\mu$ . Bernard, et al. eventually explained this discrepancy using an explicit one-loop calculation in Chiral Perturbation Theory [15].

Chiral Perturbation Theory (ChPT) can be used to solve QCD equations of nuclear processes, especially pion photoproduction near threshold. ChPT, an effective field theory, utilizes pions and nucleons as the appropriate degrees-of-freedom when performing calculations as well as making use of known symmetries in order to restrict the form of a possible interaction [16]. All of the symmetries of QCD can only be inferred into physics at the energies given by ChPT [17]. However, the results yielded by ChPT are only useful at the near threshold region. When studying charged-pion photoproduction near threshold, ChPT becomes a very useful tool in

performing multipole analysis. This is due to the fact that near threshold charged-pion production inelasticities are well removed, and multipole decomposition and model-independent predictions from ChPT converge rapidly. This allows for experimental data to provide precision tests of ChPT for energies from  $\Delta(1232)$  down to threshold. By using ChPT, the threshold values of the dominant s-wave term (the  $E_{o+}$  amplitude) for charged pion photoproduction have been predicted. When compared to values of the SAL and MAMI measurements close to threshold, the ChPT results produce good agreement between theory and experiment [18]. Theoretical work on the higher order terms beyond s-wave have been formulated, however, these have not been tested for the charged pion channel. More accurate data on the differential cross sections for charged pion photoproduction from new experiments would be required to properly test these higher order terms.

By considering the terms other than the  $E_{o+}$  multipole, more aspects of the ChPT calculations can be tested. In the case of p-wave contributions, there will be a change in the angular distribution. Measuring the differential cross sections for the pion photoproduction will provide new data to test the ChPT calculations and place constraints on associated ChPT parameters. SAL and MAMI have investigated the  $\gamma + p \rightarrow \pi^0 + p$  channel and have added extensive data to such ChPT calculations. The data analyzed is in agreement the ChPT predictions for both s- and p-waves multipoles for the reaction. Table 4.1 below shows this agreement for  $E_{o+}$  amplitudes [13]:

For the  $\gamma + p \rightarrow n + \pi^+$  channel a precision measurement has been performed at SAL with absolute uncertainty of 3% (1% statistical and 3% systematic). The purpose of the measurement at SAL, utilizing ChPT predictions, was to constrain the fundamental  $\pi NN$  coupling constant,  $f_{\pi NN}$ . The  $\pi NN$  coupling constant,  $f^2$ , equals 0.079 for the ChPT calculations in Table 4.1 [5]. This application is just one example of the benefits of ChPT when studying pion photoproduction.

Channel	ChPT ( $10^{-3}m_{\pi}^{-1}$ )	LET ( $10^{-3}m_{\pi}^{-1}$ )	Recent Experimental Values ( $10^{-3}m_{\pi}^{-1}$ )
$\gamma + p \rightarrow p + \pi^{\circ}$	-1.16	-2.3	$-1.32 \pm 0.08$
$\gamma + p \rightarrow n + \pi^{+}$	$+28.2 \pm 0.6$	$+27.6 \pm 0.2$	$+28.1 \pm 0.5$
$\gamma + n \rightarrow p + \pi^{-}$	$-32.7 \pm 0.6$	$-31.7 \pm 0.2$	$-31.5 \pm 0.8$
$\gamma + n \rightarrow n + \pi^{\circ}$	+2.6	-0.5	—

Table 4.1: ChPT, LET, and experimental values for pion photoproduction from the nucleon

## 4.2 Partial Wave Analysis

When observing pions the scattering of the generated pion is normally measured in terms of its differential cross section. A differential cross section,  $\frac{d\sigma}{d\Omega}$ , is the probability per unit solid angle that an incident particle is scattered into the solid angle  $d\Omega$  [12]. Total cross sections,  $\sigma$ , give the total probability of an event being scattered in any direction at a given energy,  $\sigma = \int \frac{d\sigma}{d\Omega} d\Omega$ . This allows for  $\frac{d\sigma}{d\Omega}$  to be viewed as being varied over the surface of a sphere, or the event as being a spherical wave. By having the outgoing particles represented by a spherical wave, it makes sense to view the incident particle as a plane wave made up of the superposition of spherical waves. The incident wave then would be  $\Psi_{inc} = Ae^{ikz} = A \sum_{\ell=0}^{\infty} j^{\ell} (2\ell + 1) j_{\ell}(kr) P_{\ell}(\cos\theta)$ , where  $A$  is a normalization constant,  $j_{\ell}(kr)$  are spherical Bessel functions, and  $P_{\ell}(\cos\theta)$  are Legendre polynomials. The expansion of the incident wave is called a partial wave expansion, where each partial wave corresponds to a specific angular momentum  $\ell$ . For pion photoproduction near threshold only  $\ell = 0$  and  $\ell = 1$  are generally considered since the s-wave and p-wave contributions are dominant. At a given photon energy, photoproduction events can occur at various angles. If the beam is unpolarized, the variance of the pion cross section is limited to  $\theta$  only. Since  $\frac{d\sigma}{d\Omega} = \frac{d\sigma^2}{d\theta d\phi}$  and there is no determined variance in  $\phi$  for unpolarized photon beams, the differential cross section will be  $\frac{d\sigma}{d\theta}$  for most photoproduction data.

Utilizing such partial wave expansions as a tool to interpret observed multipole amplitudes is called partial wave analysis. Partial wave analysis is performed by creating multipole fits to the known data points. There have been many different partial wave analyses made to study the production of pions, each of which has taken a different approach to fitting the existing data.

One such partial wave analysis (PWA) has been developed at Mainz University in Germany and is known as MAID or the Mainz Unitary Isobar Model. The MAID model was developed in 1998 and adapted to a web-based format for easy access to researchers. The first version, MAID98, used the seven most important nucleon resonances for pion photoproduction in Breit-Wigner form and a non-resonant background including the Born terms [19]. MAID98 was unitarized for each partial wave up to the threshold for double-pion production. The model then progressed into MAID2000 with the addition of an eighth resonance and the Dubna-Mainz-Taipei dynamic model being used to modify the unitarization procedure [19]. As of MAID2000, the model still had not been fitted to the entire world data set for pion photoproduction and electroproduction. Once the MAID solution was fitted, some background parameters were adjusted to the multipoles from the SAID partial wave analysis. Beginning in 2003 MAID became a full partial wave analysis program, with all parameters fitted to experimental observables as cross sections and polarization asymmetries. Also, MAID included both pion photoproduction and electroproduction data in its fits. MAID continued to progress with the addition of analysis programs for eta and kaons. MAID2005 is the most current version of the MAID PWA package.

Another PWA package is known as SAID (Scattering Analysis Interactive Dial-in) which is currently developed at the Center for Nuclear Studies at George Washington University, SAID began as a program which allowed users to access and compare databases, models, and partial wave solutions for elastic scattering. Pion photoproduction and capture ( $\pi^+ + d \rightarrow p + p$ ) reactions were also added to the SAID program

code. Early versions of SAID were available as FORTRAN program downloads. The current version of SAID is available through either an SSH or as an HTML form on the Center for Nuclear Studies website.

# Chapter 5

## This Research

### 5.1 Experiment Overview

The proposed experiment, which this research supports, is to be performed at MAX-lab located at Lund University in Sweden. The investigators of the proposed experiment are from the University of Massachusetts Dartmouth, Lund University, George Washington University, and Mainz University. The experiment is intended to be a commissioning experiment for the pion photoproduction program at MAX-lab and run for three weeks.

The experiment will measure differential cross sections of the  $\gamma + p \rightarrow n + \pi^+$  reaction with photon energies from 15–30 MeV above threshold with a photon bin width of 1 MeV. These measurements will provide new data on the pion photoproduction process at energies above threshold up to the first resonance region. Estimates of the uncertainties of the final results is 5% statistical uncertainty with comparable systematic uncertainties. The measurements of  $E_\gamma \approx 165\text{--}180$  MeV would contribute greatly to the world data set on pion photoproduction which is used by partial wave analysis such as MAID and SAID. The experiment will utilize simple targets using well understood detectors and data analysis techniques.

The reaction targets will be solid  $\text{CH}_2$  and C which will be bombarded with tagged photons. The tagger will be configured to tag photons in the 145–180 MeV

range with 430 keV resolution. The photons will be generated using an electron beam energy of 200 MeV and the end-point tagger will be used in conjunction with the SAL focal-plane detector array. Adjacent tagger channels will be added to improve statistics, resulting in the 1 MeV photon energy bins. Pions with energies below about 15 MeV will not be detected due to energy loss in the target, thus data will only result for  $E_\gamma > 160$  MeV. An additional beam energy of 250 MeV with a reduced magnetic field setting will also be used to tag photons in the 155–190 MeV range. This will better match the tagged photon range with the kinematics of the experiment [1]. The tagged photon energy range used at both energy settings includes a portion of the focal plane counters tagging photons in an energetically forbidden region. Data in these forbidden regions will be used to understand the background.

The targets will be mounted on a target ladder located 1 meter from the photon beam collimators. The ladders will be remote controlled and include an empty position to measure the room background. The pions will be detected by  $\Delta E$ -E detector telescopes placed at various angles. The detectors will be placed approximately 25 cm from the target to ensure the loss of pions due to decay-in-flight is less than 5%. The charged pions,  $\pi^+$ , events will be identified using measurements of the stopping power using a thin  $\Delta E$  and thick full-E detector telescope. When  $\Delta E$  values are plotted against the stopping power E, the pion events are clearly separated from electron and proton events. Additionally, background events would be rejected based on the measurement of the  $\pi \rightarrow \mu$  ( $\tau \sim 26$ ) ns decay. This research pertains to the angular placement of these detectors.

## 5.2 Research Overview

This research utilized the SAID interface to generate differential cross section data of various PWA. The PWA which were available changed during the course of this research. Initially, during July of 2005 the available PWA included Born-Delta,

SM95\_2GeV, D500, and the Current SAID solution. By early 2007, MAID2003 and MAID2005 PWA had been added and the D500 and Born-Delta had been removed. This allows for data from six different PWA to be compared in this research.

Initially, data was taken at various energies from pion threshold up to 180 MeV with the angle at each energy being varied from 0 to 180 degrees. The SAID interface however is not programmed to generate more than 60 points per run. To gain 1 degree resolution for each energy and PWA, data was collected at 0 to 60 degrees, 61 to 120 degrees, and 121 to 180 degree. The data was placed into one data file for the entire 0 to 180 degree range for each energy and PWA. The energy levels which were run for each PWA were 155 MeV to 180 MeV in 5 MeV increments.

Comparisons between the different PWA solutions were made by plotting the various solutions against each other. By comparing the fixed energy PWA data, similarities and differences between the PWA could be viewed at the corresponding angles. Through this analysis of the plots, areas of interest were determined for detector placements. Generally, these areas of interest were those regions where differences between the PWA fits could be resolved with new experimental data. A total of four angular positions were chosen. At these four angles, fixed angle data of cross sections was taken for the range of slightly above threshold (152 MeV) to 180 MeV. All plots were generated using the Grace plotting package.

The SAID interface also allows access to the existing experimental data points. Utilizing this feature, plots were generated showing the cross sections of all pion photoproduction data within the energy range of threshold to 180 MeV. This plot can be seen in Fig. 5.1. Additionally, showing the data from threshold to 250 MeV allows for a visual aid of the gap in pion photoproduction below 180 MeV. This gap can be seen in Fig. 5.2. The energy-angle distribution of the known data, Fig. 5.3, also shows a clear gap in the data set below 180 MeV.

To better understand the PWA fits some of the recent data points from Ahrens

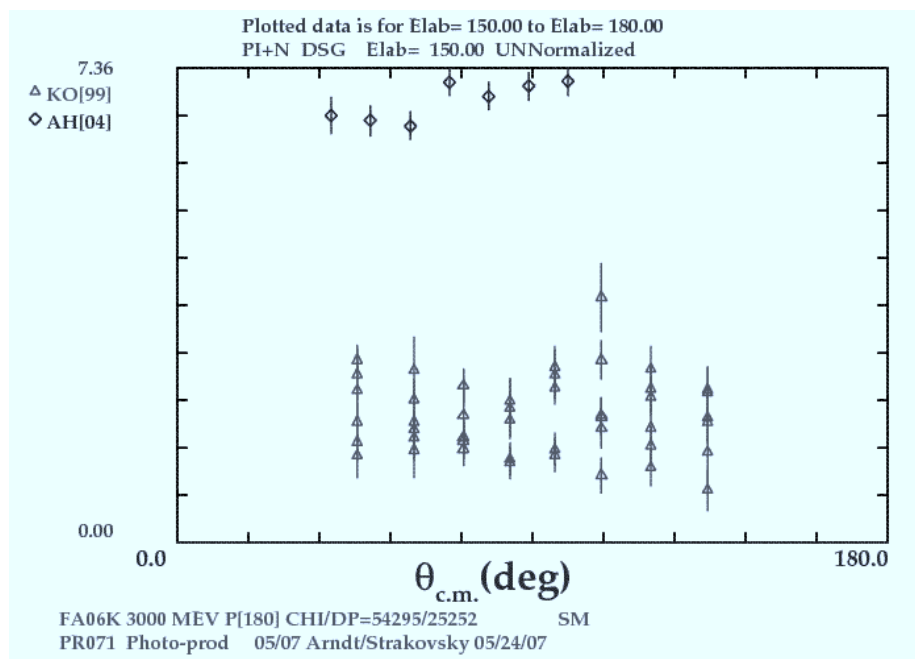


Figure 5.1: Known pion photoproduction data from threshold to 180 MeV. Generated by the SAID interface.

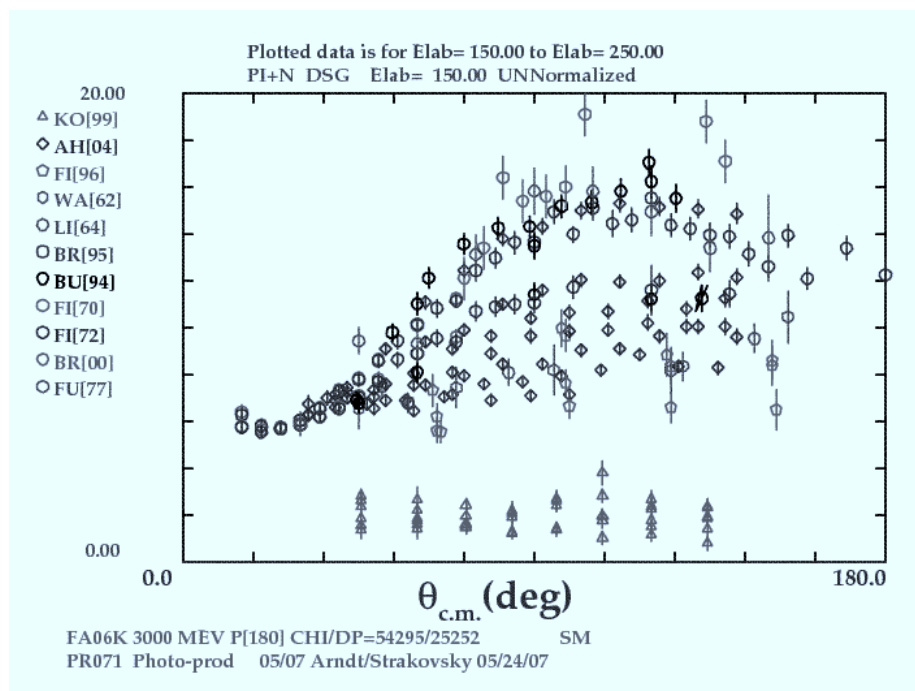


Figure 5.2: Known pion photoproduction data from threshold to 250 MeV. Generated by the SAID interface.

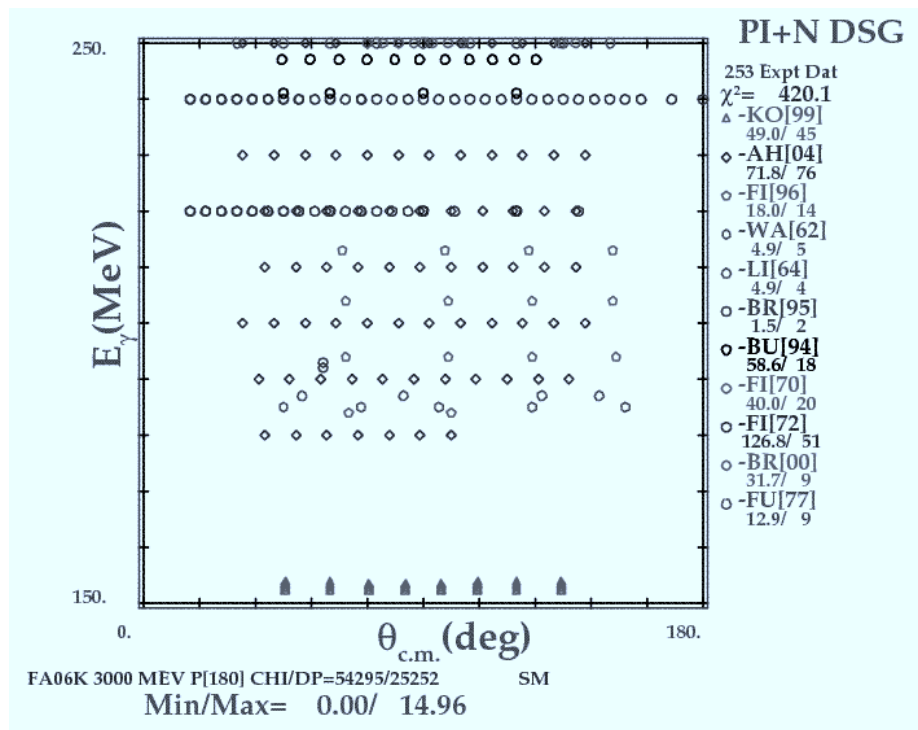


Figure 5.3: Energy-Angle distribution of known pion photoproduction data from threshold up to 250 MeV. Generated by the SAID interface.

and Korkmaz were plotted against the current SAID, MAID2003, and MAID2005 solutions. From the Korkmaz 1999 experiment the data plotted was at 153.390 MeV and 153.750 MeV. A plot of this data for 153.750 MeV can be seen in Fig. 5.4.

For Ahrens the 180 MeV data was plotted and is shown in Fig. 5.5.

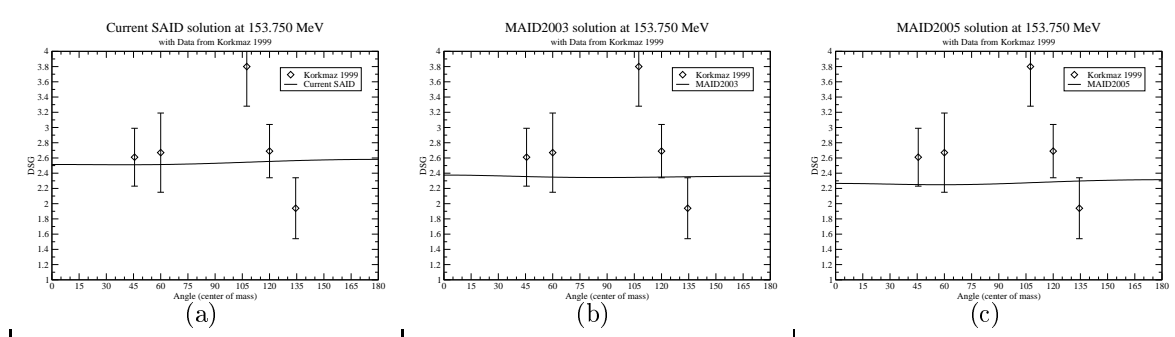


Figure 5.4: Current SAID, MAID2003, and MAID2005 with Korkmaz 153.750 MeV Data

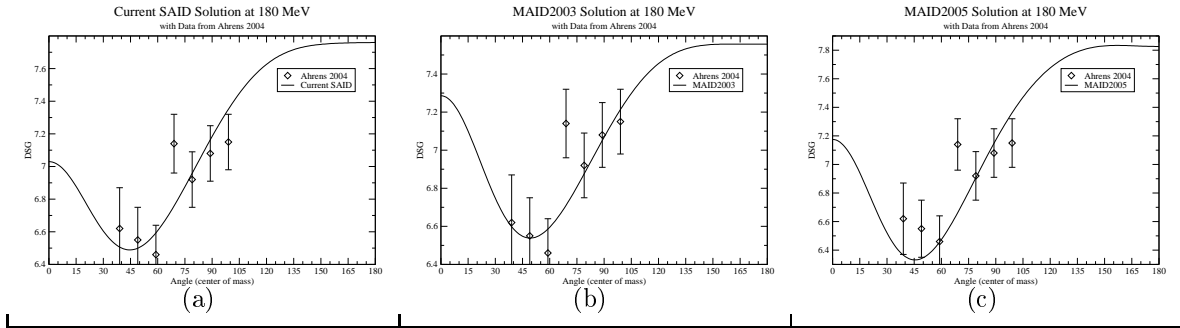


Figure 5.5: Current SAID, MAID2003, and MAID2005 with Ahrens 180.000 MeV Data

### 5.3 PWA Results

Once data was generated for each of the PWA at the energy levels between 155 MeV and 180 MeV, the PWA results for each were plotted using Grace. Grace, a descendant of Xmgr, is a WYSIWYG (What-You-See-Is-What-You-Get) plotting package for Unix. Each plot included the Born & Delta, D500, SM95\_2GeV, MAID2003, MAID2005, and current SAID PWA solutions. From these plots, areas of interest were noted where there were large differences, changes, or other unique behaviors in the various PWA solutions.

#### 5.3.1 155 MeV

For the 155 MeV plot, shown in Fig. 5.6, the cross section of both the SM95\_2GeV and Born & Delta drop off fairly quickly. The Born & Delta begins to level off at around 105 degrees as well as the SM95\_2GeV crosses below the Born & Delta value. The current said solution remains higher than the MAID2003 or MAID2005 solutions for the full angular range. After about 75 degrees however both the current SAID and MAID2005 the cross section begins to rise in value. Being the lowest energy to be investigated the 155 MeV is expected to have the least contribution from the  $\Delta$ -resonance.

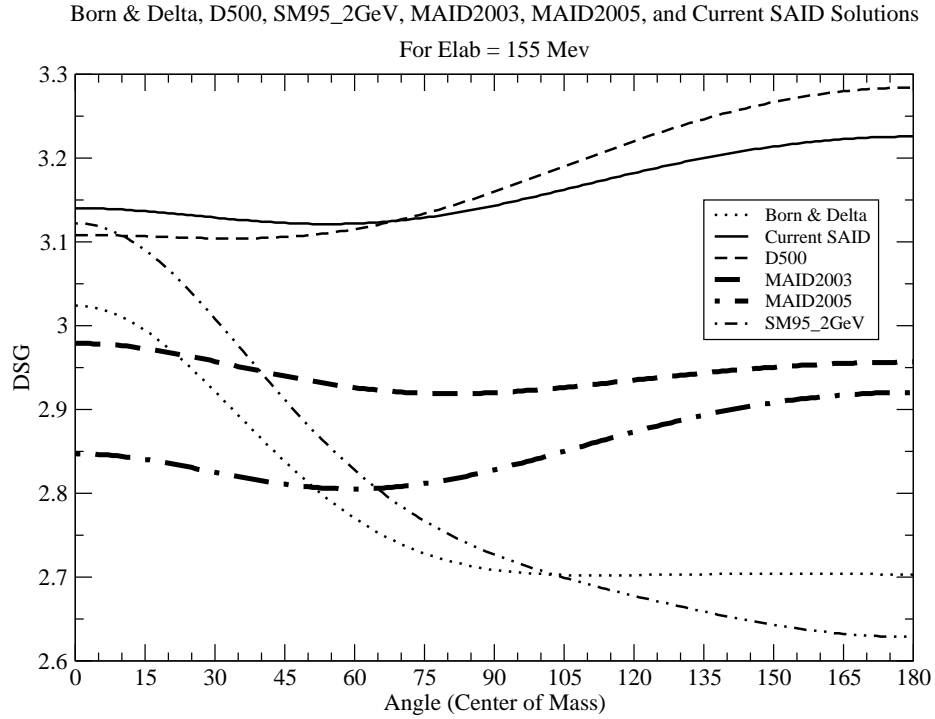


Figure 5.6: All PWA solutions at 155 MeV incident photon energy

### 5.3.2 160 MeV

In the plot of the 160 MeV solutions, shown in Fig. 5.7, the current SAID and D500 are very similar in shape and behavior. The D500 however crosses above the current SAID solution at about 75 degrees. From 45 degrees to 75 degrees in all of the solutions there appears to be a change from a decrease in cross section to an increase. Another angle of interest is 120 degrees which is approximately where the MAID2005 crosses above the MAID2003 solution. Between 105 degrees and 120 degrees the SM95\_2GeV begins to decrease as well as the Born & Delta solution rises above the SM95\_2GeV. The overall shape of the Born & Delta and the MAID2003 also show similar changes. The current SAID and MAID2005 both trend to have higher cross sections towards 180 degrees than at 0 degrees.

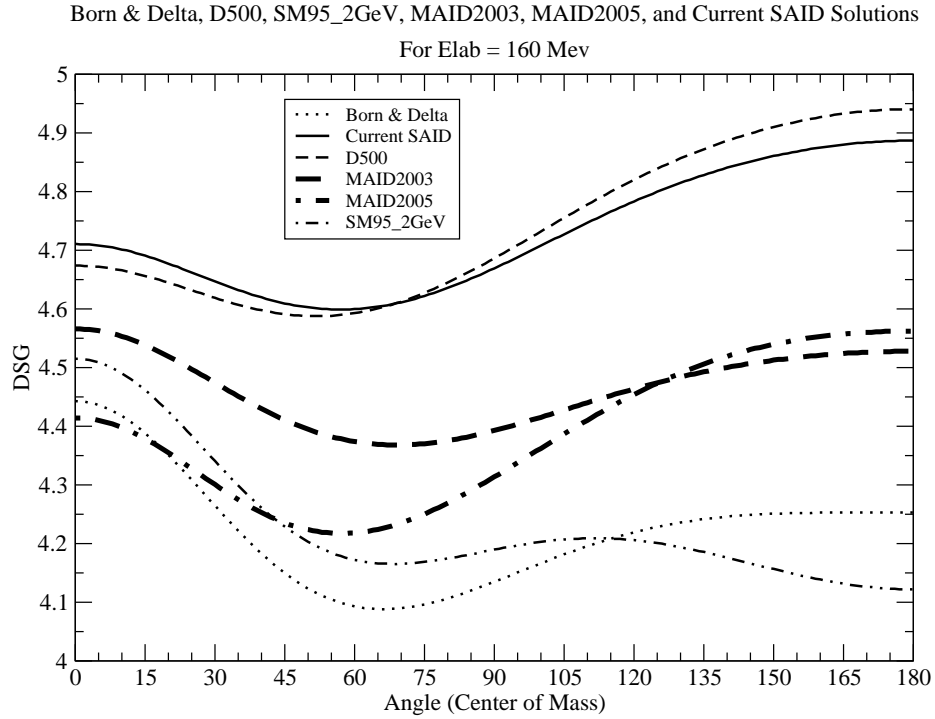


Figure 5.7: All PWA solutions at 160 MeV incident photon energy

### 5.3.3 165 MeV

The 165 MeV plot, shown in Fig. 5.8, has features similar to the 160 MeV plot. The area of change from decreasing to increasing cross section from 45 degrees to 75 degrees is more prominent. The MAID2005 solution appears to have much more variation than the MAID2003 solution did at this energy. Other than the SM95\_2GeV, the other solutions show signs of increase in the area past 120 MeV where the Born & Delta levels off. This could be due to higher order resonances beginning to have an effect.

### 5.3.4 170 MeV

Beginning with the 170 MeV plot; shown in Fig. 5.9; the current SAID, MAID2003, MAID2005, and D500 all begin to have closer cross section values. The MAID2003 also begins higher than both the current SAID and D500. Between 75 degrees and 90 degrees the MAID2005 cross section goes above the MAID2003 solution. The

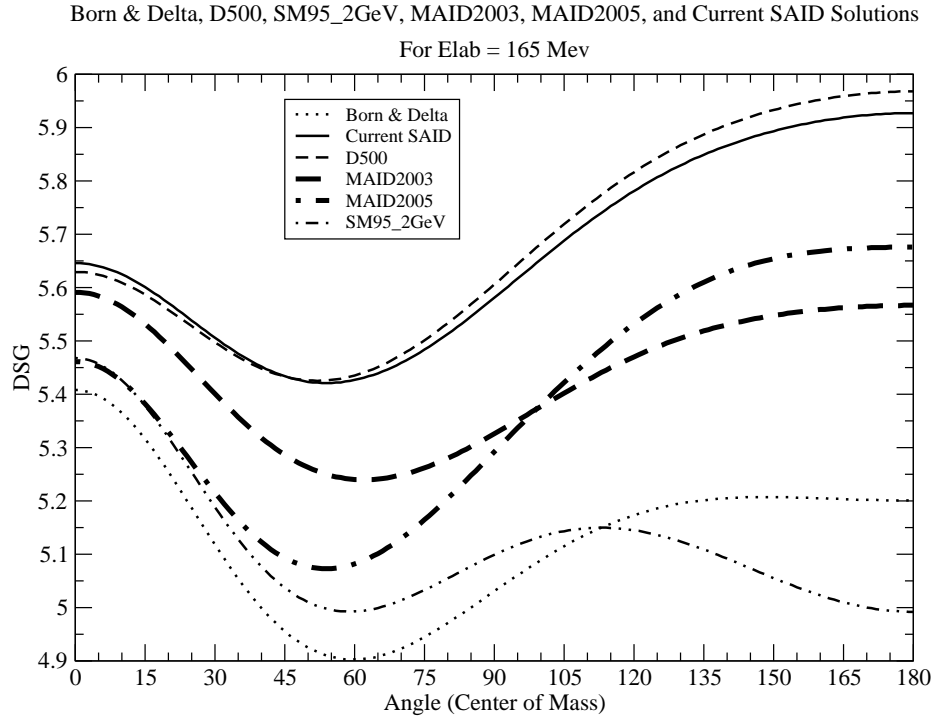


Figure 5.8: All PWA solutions at 165 MeV incident photon energy

SM95\_2GeV begins to change from increasing to decreasing between about 105 degrees and 120 degrees. In that same range all of the other PWA solutions continue to increase in cross section.

### 5.3.5 175 MeV

In the 175 MeV plot; shown in Fig. 5.10; the MAID2005, current SAID, and D500 show good agreement near 0 degrees and above 105 degrees. The largest difference between these three solutions occurs at about 45 degrees, which is the lowest cross section for the MAID2005. The MAID2005 crosses above the MAID2003 at around 75 degrees. The Born & Delta begins to show signs of decrease slightly after 120 degrees. The SM95\_2GeV continues to match the Born & Delta closely from 0 degrees up to 105 degrees, after which it decreases steadily. The SM95\_2GeV appears to not have too much dependence on higher order resonances.

Born & Delta, D500, SM95\_2GeV, MAID2003, MAID2005, and Current SAID Solutions  
For Elab = 170 Mev

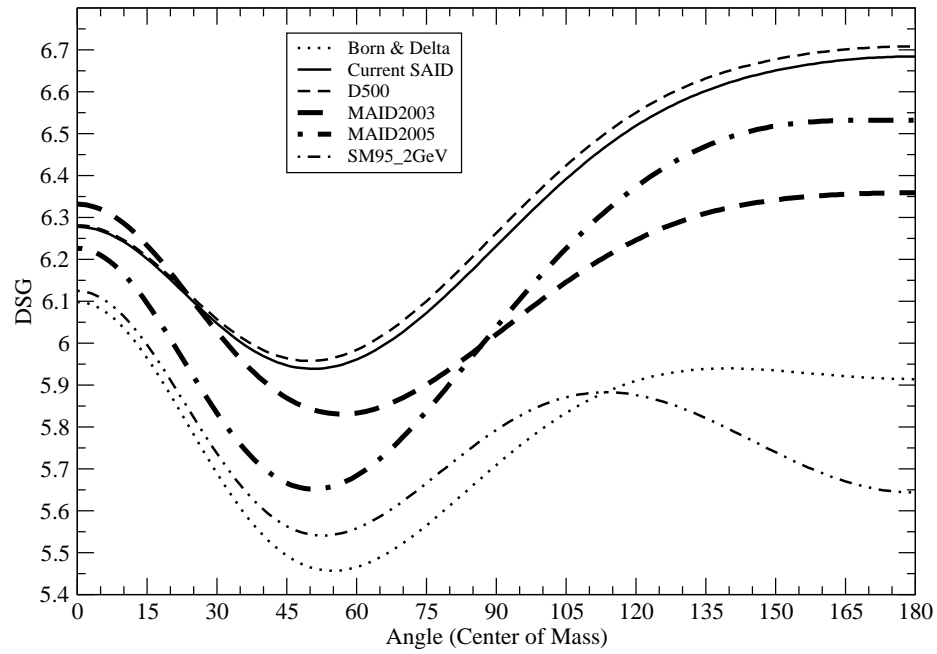


Figure 5.9: All PWA solutions at 170 MeV incident photon energy

Born & Delta, D500, SM95\_2GeV, MAID2003, MAID2005, and Current SAID Solutions  
For Elab = 175 Mev

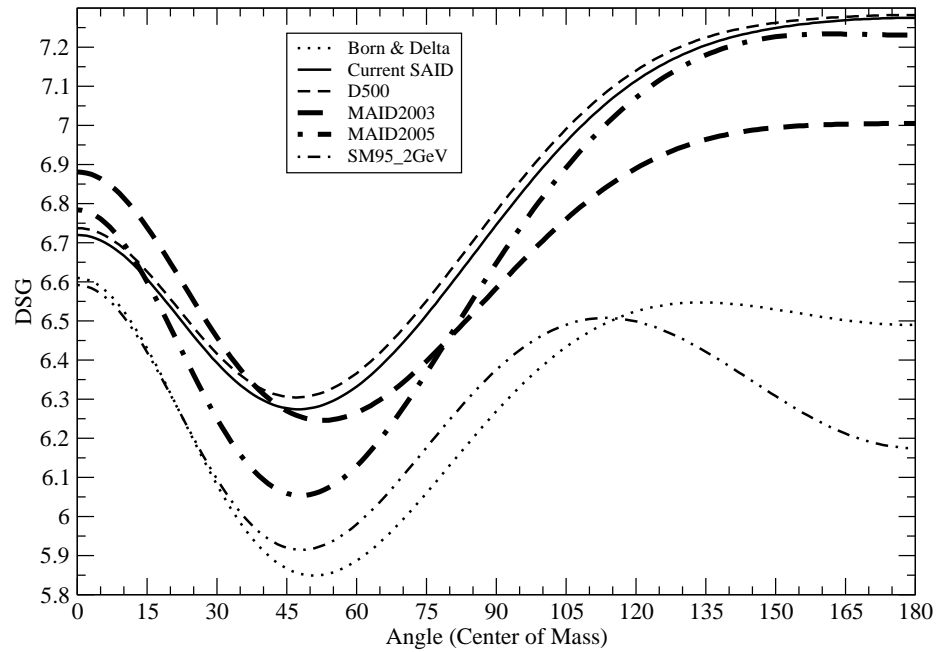


Figure 5.10: All PWA solutions at 175 MeV incident photon energy

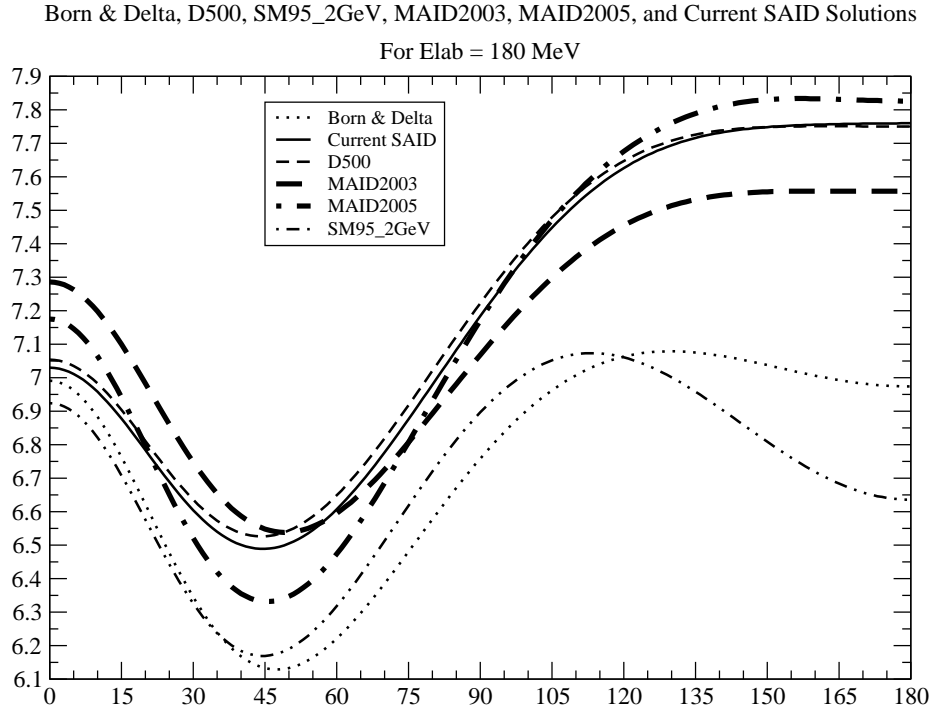


Figure 5.11: All PWA solutions at 180 MeV incident photon energy

### 5.3.6 180 MeV

The final energy plot which was view was the 180 MeV, shown in Fig. 5.11. The cross sections for the Born & Delta and SM95\_2GeV are significantly lower above 105 degrees. Most of the PWA solutions appear to have their lowest values around 45 degrees. Again, the MAID2003 and MAID2005 cross at about 75 degrees, with MAID2005 having higher cross sectional values above that angle. By about 120 degrees, the current SAID, MAID2003, MAID2005, and the D500 have begun to level off. As the energy increase it appears that each of the recent solutions follow similar trends with relatively close values for cross sections.

## 5.4 Detector Placement

The SAID interface handles all angles as  $\theta_{\text{cm}}$ , angles in the center of mass frame. Therefore all the angles of interest would need to be converted from the center of mass

frame to the laboratory frame for the proper detector placements in the laboratory. Transformations between the center of mass frame and the laboratory frame include dependencies on the particle energies. For this discussion of placement however it is satisfactory to consider placement in terms of  $\theta_{\text{cm}}$ , considering that the pions will be produced so close to threshold.

The criteria for determining the detector placements included finding angles where the PWA solutions had large differences as well as areas where the solutions had good agreement. Utilizing this criteria to determine the placement of the four detectors, will help to gain data which would aid in the evolution of the PWA solutions.

#### 5.4.1 45 degrees

The first angle which is recommended for detector placement is 45 degrees. At about 45 degrees the cross section values begin to approach their lowest values. Also, the largest difference between the MAID2005 and the current SAID occurs around this angle in the 175 MeV (Fig. 5.10) and 180 MeV (Fig. 5.11) plots. The cross section at 45 degrees was plotted from 152 MeV to 180 MeV in Fig. 5.12. This plot would aid in visually understanding the energies at which the cross section values are closest and most separated.

#### 5.4.2 75 degrees

Similar to the 45 degree detector placement is the recommended angle of 75 degrees. At about 75 degrees the cross section values have begun to rise from their lowest values. Furthermore, by placing a detector at 75 degrees it will allow for observation of cross sections on both sides of the change from decreasing to increasing values. Even in the lower energy plots, such as 155 MeV (Fig. 5.6), the values of MAID2005 and the current SAID begin to rise. Also, around 75 degrees the MAID2005 rises above the MAID2003 in most of the higher energy plots. The 75 degree cross section

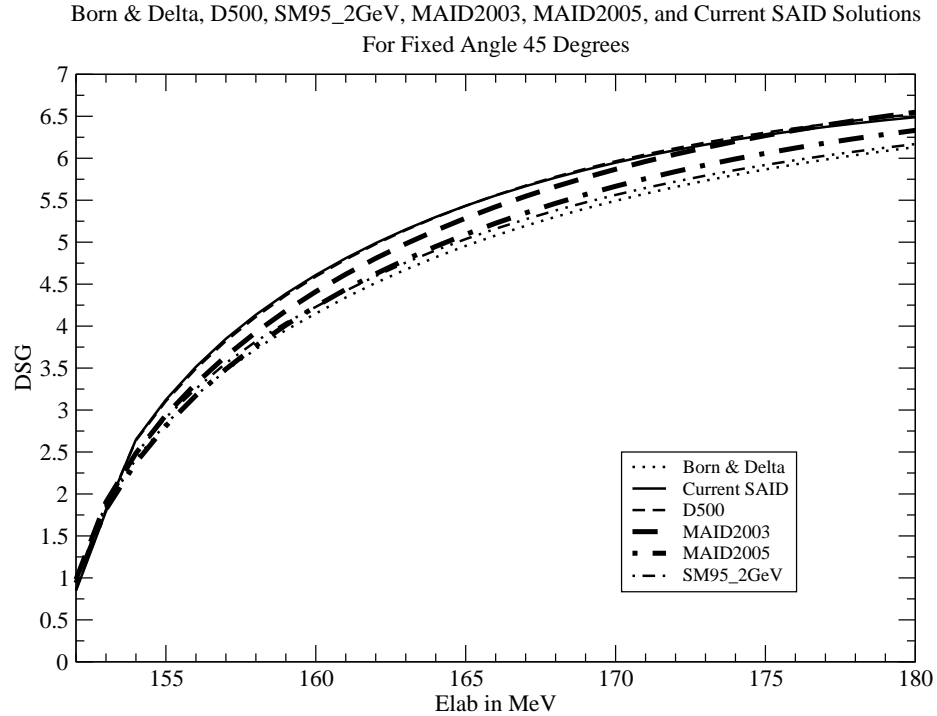


Figure 5.12: Cross sections at 45 degrees for all PWA solutions from 152 MeV to 180 MeV

is shown in Fig. 5.13.

### 5.4.3 105 degrees

The third recommended detector placement angle is at 105 degrees. Both the Born & Delta and SM95\_2GeV have peaks or plateaus, across most of the energies plotted, beginning at 105 degrees. Also, in the higher energy plots MAID2003, MAID2005, and the current SAID have a good agreement in cross section values with similar trends. The 105 degree cross section plot is shown in Fig. 5.14.

### 5.4.4 120 degrees

The fourth and final recommended detector placement angle is at 120 degrees. By 120 degrees most of the PWA solutions have leveled off at the higher energies. In the 180 MeV plot (Fig. 5.11) the Born & Delta begins to show signs of a shallow decrease at about 120 degrees. Also, around 120 degrees the SM95\_2GeV cross section drops

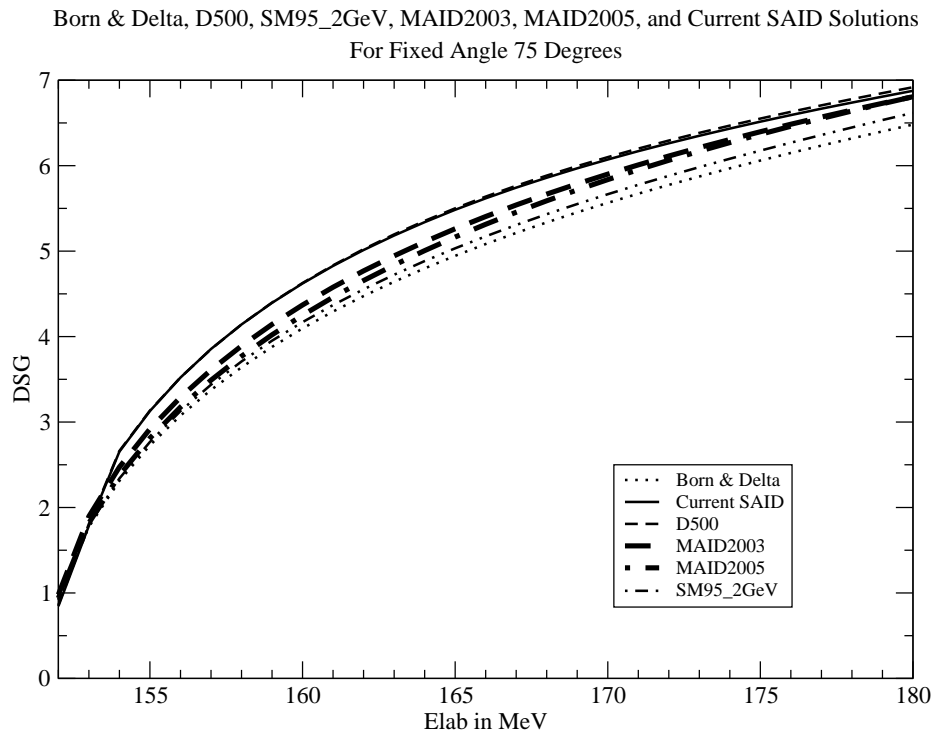


Figure 5.13: Cross sections at 75 degrees for all PWA solutions from 152 MeV to 180 MeV

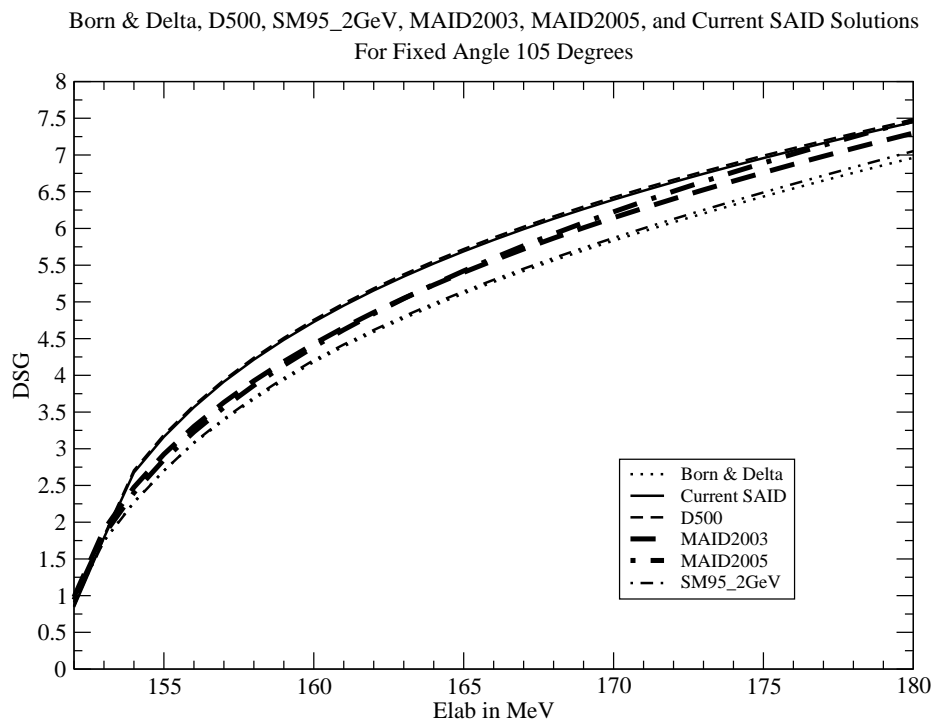


Figure 5.14: Cross sections at 105 degrees for all PWA solutions from 152 MeV to 180 MeV

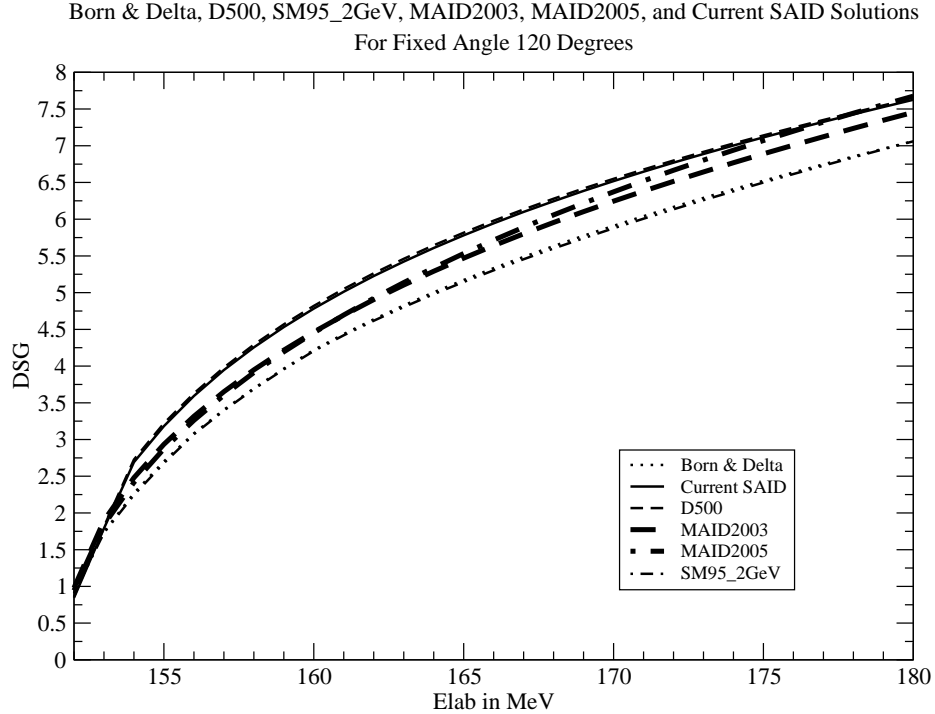


Figure 5.15: Cross section at 120 degrees for all PWA solutions from 152 MeV to 180 MeV

below the Born & Delta solution. The 120 degree cross section is shown in Fig. 5.15.

## 5.5 Conclusions

The purpose of this research was to analyze the current PWA solutions to determine the optimum detector placement for an upcoming experiment at MAX-lab at Lund University. The experiment will investigate pion photoproduction from tagged photons near the charged  $\pi^+$  threshold up to 180 MeV. A total of six different PWA solutions were investigated in the desired energy range including the current SAID, MAID2003, MAID2005, SM95\_2GeV, D500, and Born & Delta fits. From the analysis of the various PWA solutions available through the SAID interface the four recommended angular placements for the detectors are 45 degrees, 75 degrees, 105 degrees, and 120 degrees in the center of mass frame. The placement of detectors at these angles will provide useful data in the desired energy range of threshold up to

180 MeV. Acquired data points could help to distinguish which PWA solutions are closest to observations.

## Appendix A

### PWA Solutions at Incremental Energies

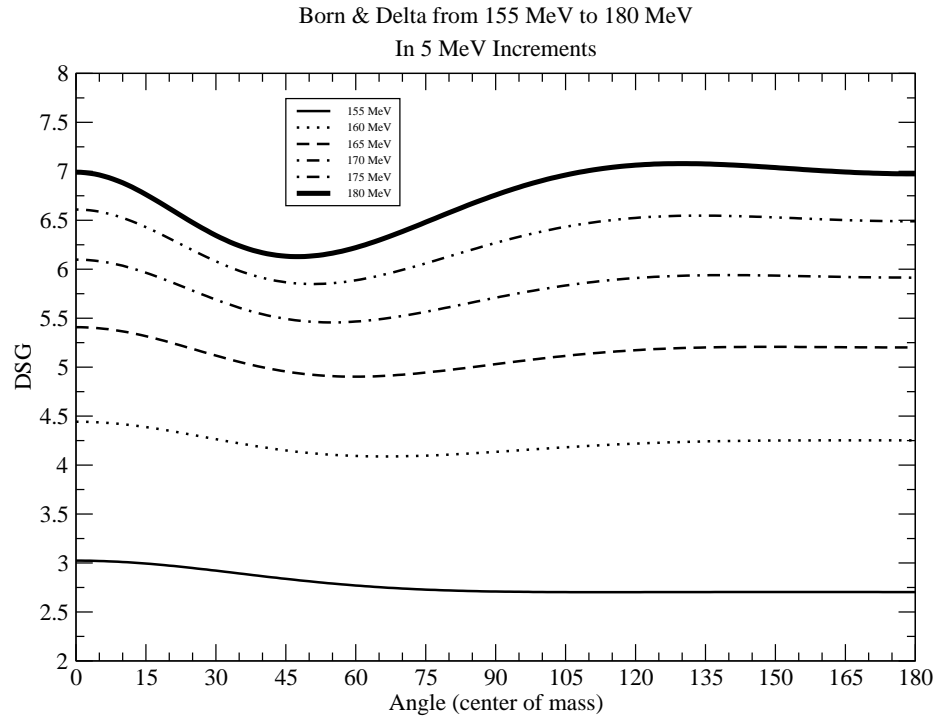


Figure A.1: Born & Delta PWA solution at 5 MeV incremental energies from 155 MeV to 180 MeV

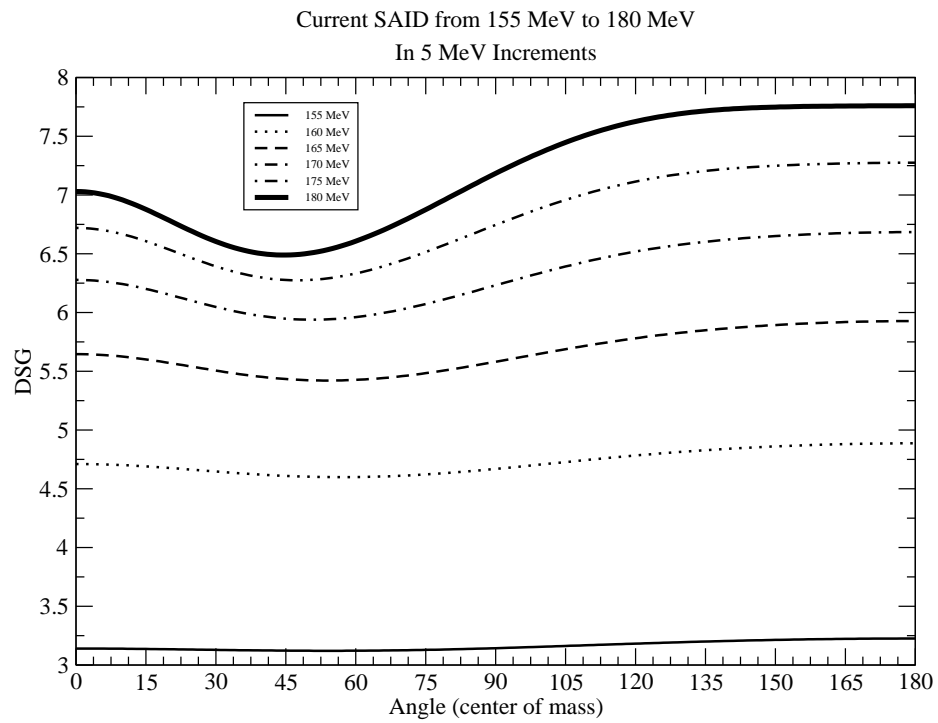


Figure A.2: Current SAID PWA solution at 5 MeV incremental energies from 155 MeV to 180 MeV

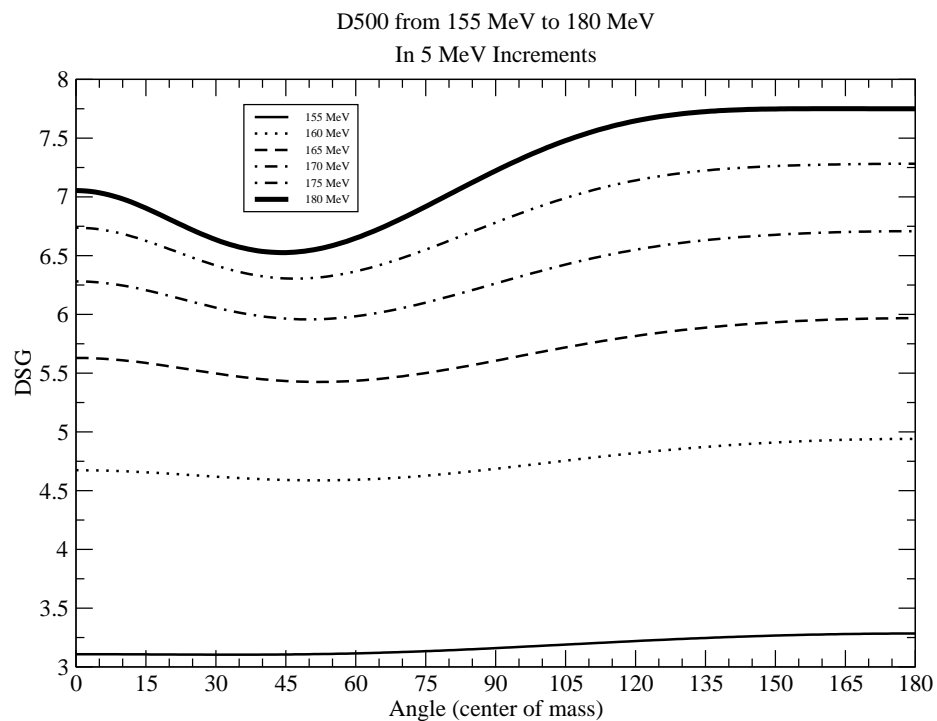


Figure A.3: D500 PWA solution at 5 MeV incremental energies from 155 MeV to 180 MeV

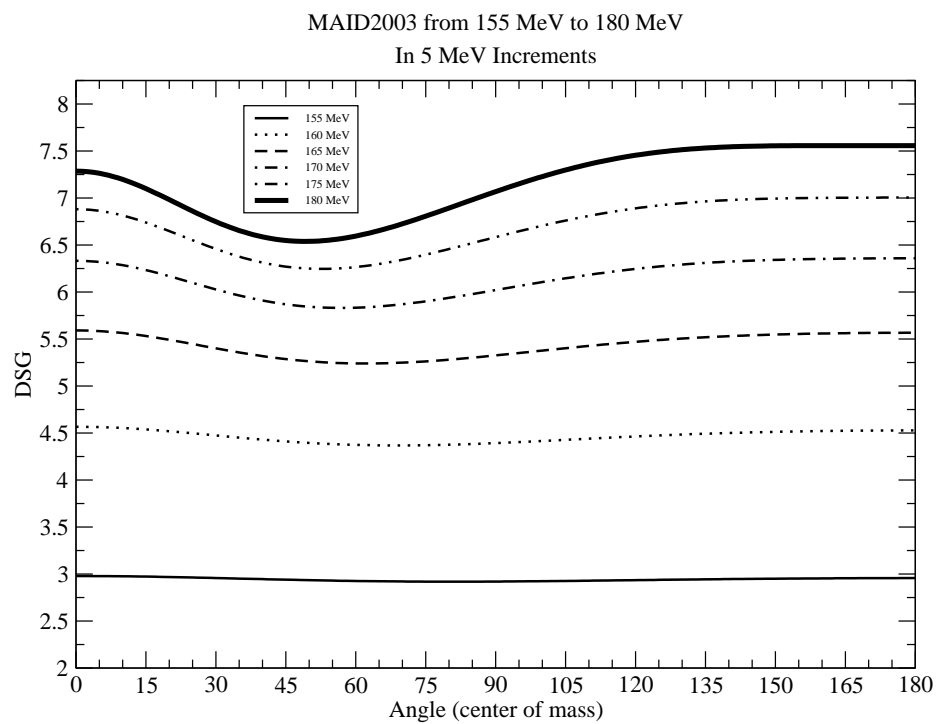


Figure A.4: MAID2003 PWA solution at 5 MeV incremental energies from 155 MeV to 180 MeV

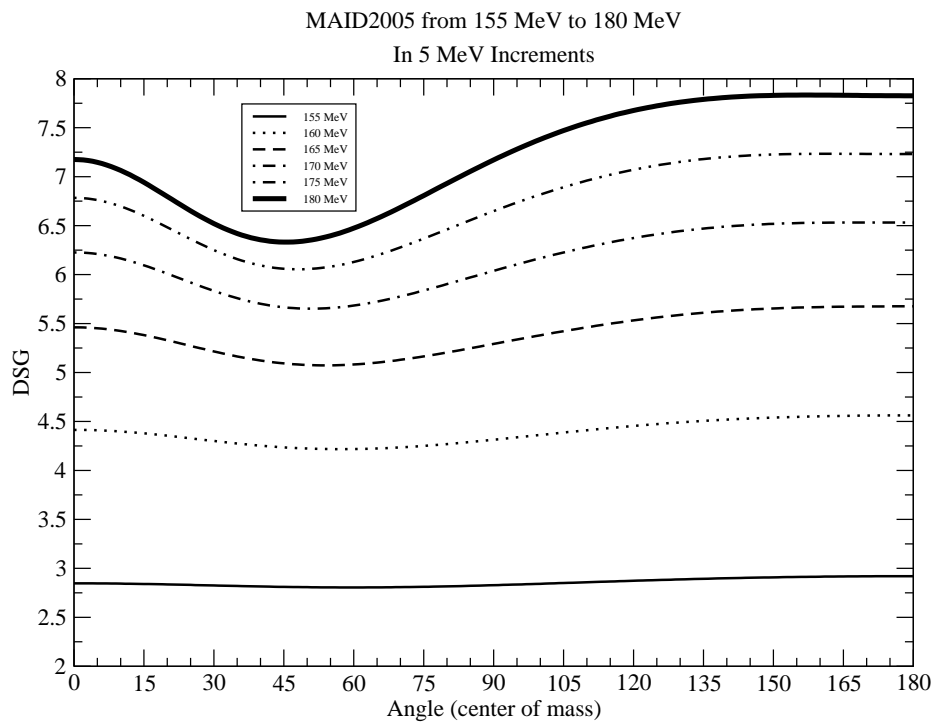


Figure A.5: MAID2005 PWA solution at 5 MeV incremental energies from 155 MeV to 180 MeV

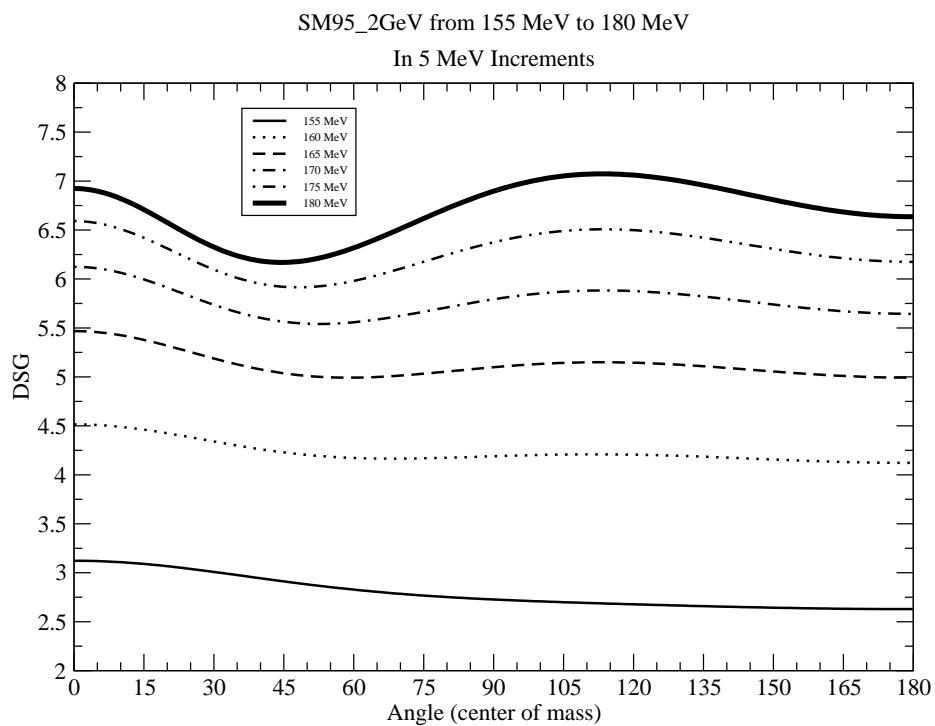


Figure A.6: SM95\_2GeV PWA solution at 5 MeV incremental energies from 155 MeV to 180 MeV

## References

- [1] G.V. O’Rielly et al., *Charged Pion Photoproduction from Threshold up to the First-Resonance Region*, 2004.
- [2] K. Heyde, *Basic Ideas and Concepts in Nuclear Physics*, Institute of Physics Publishing 1999.
- [3] P.D. Barnes et al. editors, *Meson Nuclear Physics- 1976 Carnegie-Mellon Conference*, American Institute of Physics 1976.
- [4] L. Tiator and S. Kamalov, *MAID Analysis Techniques*, 2006.
- [5] R.A. Arndt et al., *Analysis of Pion Photoproduction Data*, 2002.
- [6] H. Yukawa, *On the Interaction of Elementary Particles*, Proc. Phys.-Math. Soc. Japan, 17, p. 48, 1935.
- [7] C. Anderson and S. Neddermeyer, *Note on the Nature of Cosmic-Ray Particles*, Physical Review, Vol. 51, p. 884, 1937.
- [8] R. Marshak and H. Bethe, *On the Two-Meson Hypothesis*, Physical Review, Vol. 72, p. 506, 1947.
- [9] C. M. G. Lattes, G. P. S. Occhialini, and C. F. Powell, *Observations on the Tracks of Slow Mesons in Photographic Emulsions*, Nature, Vol. 160, p. 453, 1947.
- [10] J. Symons et al., *Opportunities in Nuclear Science: A Long-Range Plan for the Next Decade*,  
[http://www.sc.doe.gov/henp/np/nsac/docs/LRP\\_5547\\_FINAL.pdf](http://www.sc.doe.gov/henp/np/nsac/docs/LRP_5547_FINAL.pdf)
- [11] R.E. Marshak, *Meson Physics*, McGraw-Hill 1952.
- [12] Kenneth S. Krane, *Introductory Nuclear Physics*, John Wiley & Sons 1988.
- [13] Kevin G. Fissum, *Inclusive Photoproduction of Positive Pions*, Ph.D. Thesis, University of Saskatchewan 1993.
- [14] A Nagl et al., *Springer Tracts in Modern Physics Volume 120: Nuclear Pion Photoproduction*, Springer-Verlag 1991.

- [15] G.V. O’Rielly, Experimental Proposal NP014 to MAX-lab, 2004.
- [16] E. Korkmaz et al., *Measurement of the  $\gamma p \rightarrow \pi^+ n$  Reaction Near Threshold*, Physical Review Letters 83, 3609, 1999.
- [17] O. Hanstein, et al., *A Dispersion Theoretical Approach to the Threshold Amplitudes of Pion Photoproduction*, 1996.
- [18] N.R. Kolb, *Near-Threshold Pion Photoproduction at the Saskatchewan Accelerator Laboratory*, 1999.
- [19] O.Hanstein, et al., *Multipole analysis of pion photoproduction based on fixed  $t$  dispersion relations and unitary*, 1997.
- [20] B.H. Bransden and R. Gordon Moorhouse, *The Pion-Nucleon System*, Princeton University Press 1973.
- [21] N.R. Kolb, *Photonuclear Physics at the Saskatchewan Accelerator Laboratory*, 1999.